




Imaging Microstructural Damage and Alveolar Bone Loss in Rats Systemically Exposed to Methylmercury: First Experimental Evidence

Géssica de Oliveira Lopes¹ · Walessa Alana Bragança Aragão¹ · Leonardo Oliveira Bittencourt¹ · Bruna Puty¹ · Armando Pereira Lopes² · Sávio Monteiro dos Santos³ · Marta Chagas Monteiro³ · Edivaldo Herculano Corrêa de Oliveira^{4,5} · Márcia Cristina Freitas da Silva¹ · Rafael Rodrigues Lima¹ 

Received: 27 August 2020 / Accepted: 12 November 2020 / Published online: 6 January 2021
© Springer Science+Business Media, LLC, part of Springer Nature 2021

Abstract

The alveolar bone is an important mineralized structure of the periodontal support apparatus, and information about the methylmercury (MeHg) effects on the structural integrity is scarce. Therefore, this study aimed to investigate whether systemic, chronic, and low-dose exposure to MeHg can change the alveolar bone microstructure of rats. Adult Wistar rats ($n = 30$) were exposed to 0.04 mg/kg/day of MeHg or vehicle through intragastric gavage. The animals were euthanized after 60 days, and blood samples were collected for trolox equivalent antioxidant capacity (TEAC), glutathione (GSH), lipid peroxidation (LPO), and comet assays. The mandible of each animal was collected and separated into hemimandibles that were used to determine the total Hg level in the bone and to analyze microstructural damage and alveolar bone loss in terms of trabecular number (Tb.N), trabecular thickness (Tb.Th), bone volume fraction (BV/TV), and exposed root area of the second molars. MeHg exposure triggered oxidative stress in blood represented by lower levels of GSH and TEAC and the increase in LPO and DNA damage of the blood cells. High total Hg levels were found in the alveolar bone, and the microstructural analyses showed a reduction in Tb.N, Tb.Th, and BV/TV, which resulted in an increase in the exposed root area and a decrease in bone height. Long-term MeHg exposure promotes a systemic redox imbalance associated with microstructural changes and alveolar bone loss and may indicate a potential risk indicator for periodontal diseases.

Keywords Methylmercury · Periodontium · Alveolar bone loss · MicroCT · Rats

Introduction

Exposure to mercury (Hg) is considered a public health problem since it may cause harmful effects on the human body

even at low concentrations [1]. All Hg chemical forms found in nature are considered toxic, and the toxicity level is dependent on dosage, form, and exposure time [2–4]. Methylmercury (MeHg) is considered the most harmful form due to bioaccumulation/biomagnification processes and the triggering of physiological and biochemical imbalances in humans and animal models [5–9]; however, effects on the oral cavity and associated structures are scarce [10, 11].

The systemic exposure to MeHg may affect several physiological functions [3, 12–14]. Recently, our research group has shown the toxic effects of systemic, chronic, and low-dose exposure to MeHg on the salivary glands, which play a key role in the homeostasis of the oral cavity [5, 10, 11].

The toxicity of MeHg on bone tissue was shown in studies with fish, in which changes in bone metabolism were observed, with possible inhibition of osteoblast and osteoclast activity [15, 16]. In rodents, evidence on the effects of MeHg on bone tissue is scarce, although there is a study with a prenatal exposure model that revealed changes in the fetal growth pattern and delay in the ossification process [17].

✉ Rafael Rodrigues Lima
rafalima@ufpa.br; labef.icb.ufpa@gmail.com

¹ Laboratory of Functional and Structural Biology, Institute of Biological Sciences, Federal University of Pará, Augusto Corrêa Street N. 01, Guamá, Belém, Pará 66075-110, Brazil
² School of Dentistry, Institute of Health Sciences, Federal University of Pará, Belém, Brazil
³ Laboratory of Clinical Immunology and Oxidative Stress, Pharmacy Faculty, Institute of Health Sciences, Federal University of Pará, Belém, Brazil
⁴ Cytogenetics and Tissue Culture Laboratory, Evandro Chagas Institute, Ananindeua, Brazil
⁵ Exact and Natural Sciences Institute, Federal University of Pará, Belém, Brazil

Thus, there is no evidence in the literature regarding the possible effects of MeHg on the alveolar bone, using a model of chronic exposure to low doses.

The alveolar bone presents unique and specific characteristics that are necessary to provide physiological support for the dental activity, distinguishing itself from other long bones. It plays a fundamental role in the dispersion of the occlusal force received in the tooth to the rest of the oral support tissues [18]. It has distinct physiological and histological characteristics from other long bones and tissue dynamism, by deriving from the cells of the neural crest, suffering constant bone remodeling according to the stimulus (which can be local or systemic) directly influencing oral homeostasis [19, 20].

In view of the specificities of the alveolar bone tissue and its important function in the periodontal support device (periodontium) [21], this study aimed to investigate whether systemic, chronic, and low-dose exposure to MeHg can change the alveolar bone microstructure in rats. The hypothesis tested in this study was that systemic exposure to MeHg increases Hg levels in the bone inducing changes in the microstructure and results in alveolar bone loss (in height), which is an important parameter of periodontal health.

Materials and Methods

Animals and Experimental Groups

After receiving approval by the Ethics Committee on Animal Experimentation Research of the Federal University of Pará (CEPAE #225–14), 30 male and ninety-day-old Wistar rats (*Rattus norvegicus*) were maintained in cages with 5 animals each at 25 °C on a 12-h dark/light cycle and received balanced food and water *ad libitum*. Animals in the exposed group ($n = 15$) were intoxicated with 0.04 mg/kg/day of MeHg chloride (Sigma-Aldrich, Saint Louis, MO, USA) solubilized in oil, while animals in the control group ($n = 15$) only received similar volumes of oil. All animals were exposed for 60 days through intragastric gavage according to a protocol adapted from Kong et al. [22] and validated in previous studies from our research group [5, 10, 11]. The animals were weekly weighed for MeHg dose adjustment and body mass determination. In accordance with Kong et al. [22] and our previous studies mentioned above, this dose administered represents a model of populations chronically exposed to this metal.

Sample Collection

This research included biochemical and genotoxic analyses of peripheral blood, which aimed to assess the systemic damages triggered by MeHg toxicity. Additionally, the bone analyses aimed to investigate the effects of MeHg on the alveolar bone.

After 60 days of exposure, the animals were anesthetized with a combined solution of ketamine (90 mg/kg) and xylazine (9 mg/kg) and blood samples were collected through an intracardiac puncture. The blood samples were stored in tubes with 50 μL of 5% ethylenediaminetetraacetic acid (EDTA) and centrifuged at 3000 rpm for 10 min, except for one aliquot from each sample that was kept fresh and without centrifugation for comet assay and reduced glutathione (GSH) quantification, respectively. Then, plasma was collected and stored in microtubes at -80 °C. Plasma samples were analyzed for thiobarbituric acid reactive substances (TBARS) and Trolox equivalent antioxidant capacity (TEAC). The results of the biochemical analyses in the blood were expressed as a percentage of the control.

Each animal mandible was collected and separated into hemimandibles that were used to respectively determine the total Hg level in the alveolar bone and to analyze microstructural damage and alveolar bone loss. All experimental steps are summarized in Fig. 1.

Oxidative Biochemistry Analyses

Reduced Glutathione (GSH)

The reduced GSH content was determined according to adapted Ellman's method [23]. For the first measurement, 20 μL of total blood were diluted on 180 μL of distillate water in order to induce hemolysis. After that, an aliquot (20 μL) of the hemolysate was placed in a tube with 20 μL of distilled water plus 3 mL of PBS-EDTA buffer solution (pH 8.0). Then, 5,5'-ditiobis-2-nitrobenzoic acid (DTNB; 0.47 mmol) was added to the solution and the second measurement was performed after 3 min. The results were expressed in $\mu\text{g}/\text{mL}$ then converted into percentage (%) of control.

Trolox Equivalent Antioxidant Capacity (TEAC)

The TEAC was determined according to a non-specific method adopted by Rufino et al. [24]. Potassium persulfate (2.45 mM) was added to 2,2'-azino-bis(3-ethylbenzothiazoline)-6-sulfonic acid (ABTS; 7 mM) and incubated at room temperature for 16 h to produce ABTS+radical. The working solution was prepared with ABTS+radical and phosphate-buffered saline (PBS) solution (pH 7.2) to obtain an absorbance of 0.7 ± 0.02 at 734 nm. Subsequently, 30 μL plasma or Trolox standard (standard curve) was added to 2970 μL of ABTS working solution and the absorbance was read after 5 min. The absorbances were measured in triplicate, calculated by following a standard curve with Trolox [25] and the total antioxidant capacity in plasma was expressed in $\mu\text{mol}/\text{L}$ then converted into percentage (%) of control.

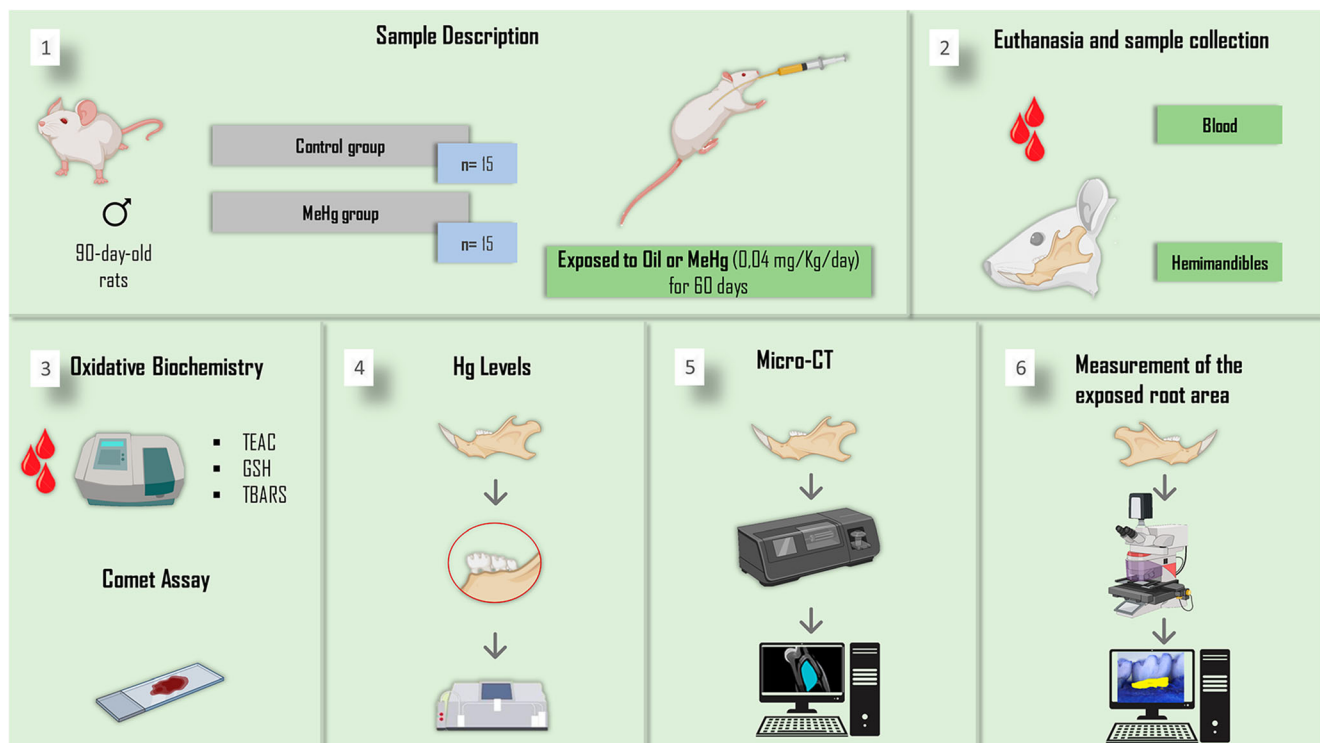


Fig. 1 (1) Sample description. (2) Blood and hemimandible collection. (3) Oxidative biochemistry analyses and comet assay. (4) Determination of Hg level. (5) Microtomography. (6) Alveolar bone loss analyses

Thiobarbituric Acid Reactive Substances (TBARS)

The TBARS determination was used to measure the lipid peroxidation (LPO), as described by Kohn et al. (1994) and modified by Percário et al. [26, 27]. The LPO produces malondialdehyde (MDA) that reacts with thiobarbituric acid (TBA) and generates a chromophore. Briefly, 1 mL of TBA (10 nM) was added to 100 μ L of samples and incubated at 94 $^{\circ}$ C for 1 h. The samples were cooled; 4 mL of n-butanol was added to each sample that was homogenized and centrifuged at 2500 rpm for 10 min. The organic phase (3 mL) was read by spectrophotometry at 535 nm and TBARS concentration was expressed in μ mol/L then converted into percentage (%) of control.

Comet Assay

The deoxyribonucleic acid (DNA) damage was analyzed by the alkaline comet assay described by Singh and Stephens [28], also called single-cell gel electrophoresis (SCGE). An aliquot of blood (20 μ L) collected from the animals exposed to MeHg was homogenized with 120 μ L of low-melting temperature agarose and added to slides pretreated with agarose layer. After drying, slides were incubated in lyse solution (in M: 2.5 NaCl, 0.1 EDTA, 0.01 Tris, and 1% Triton X-100) and maintained overnight at 4 $^{\circ}$ C. Next, the slides were placed into the electrophoresis solution (in mM: 300 NaOH, 1 EDTA; pH 13) for 20 min for DNA unwinding. Electrophoresis was

conducted for 20 min at 30 V (1 V/cm) and 300 mA. The slides were neutralized with 0.4 M Tris buffer (pH 7.5), stained with DAPI (Enzo Life Sciences, NY, USA), and analyzed with fluorescence microscopy (Axio Imager Z2, Carl Zeiss, Germany) connected to a digital image processing software (Axiovision 4.8, Carl Zeiss). Two slides per animal and 50 cells per slide were automatically analyzed through specific software (Komet 7, Andor, UK). DNA damage was expressed as the length of the comet tail in percentage.

Hg Level

The total Hg level analysis in the alveolar bone followed the method adopted by Suzuki et al. [29], in which 0.5 g maximum of wet weight per sample is determined. The method involves the reduction of Hg^{2+} ions in the sample solution with stannous chloride to generate elemental Hg vapor (Hg^0), which is measured by a cold vapor atomic absorption spectrophotometer (Hg-201 Semi-Automated Mercury Analyzer, Sanso Seisakusho Co., Japan). The values per animal were expressed in μ g/g, tabulated and submitted to statistical analysis.

Micro-computed Tomography (Micro-CT)

Non-demineralized specimens were scanned by a cone-beam micro-CT system (Skyscan 1172, Bruker, Belgium) according

to Hassumi et al. [30]. The X-ray generator was operated at an accelerated potential of 60 kV with a beam current of 165 μ A, exposure time of 650 ms per projection, and at a voxel size of $6 \times 6 \times 6$ mm. A volume of interest (VOI–prismatic section) was outlined from the apexes of all roots of second molars (touching the roots surfaces in all images of the coronal dataset) and measured with the aid of an image processing software (DataViewer, Bruker). The following parameters were analyzed: trabecular number (Tb.N), trabecular thickness (Tb.Th), and bone volume fraction (BV/TV). Such parameters allow the evaluation of bone quality in three dimensions, allowing a detailed description of structural variation. Rendered reconstructions of the microtomographic sections were also obtained by using a 3D software (CTAn, Bruker).

Exposed Root Area

The measurement of the area between the cementoamel junction (CEJ) and alveolar bone crest of second molars was used for better delimitation of the area to be evaluated and as a sensitive parameter of alveolar bone loss [31]. The hemimandibles were immersed in 8% sodium hypochlorite for 4 h to remove soft tissue remnants, washed in running water, immediately dried, and immersed in 1% methylene blue (Sigma-Aldrich) to better delineate the CEJ [32]. Subsequently, images of the exposed area of the lingual surface of second molars were obtained with a stereomicroscope (M205A, Leica, Wetzlar, Germany) and imaging software (LAS-X, Leica). The limits of the images were the CEJ, alveolar bone crest, and mesial and distal surfaces of the second molars.

Statistical Analyses

The sample size calculation was performed considering the exposed root area variable with mean difference of 0.1 and standard deviation of 0.1 between groups. The power of the test was considered 80%, alpha level of 0.05, and allocation

rate of 1 : 1, resulting in 15 animals per group. The data distribution of each group was tested by the Shapiro–Wilk test. Student's *t* test was applied for the variables normally distributed. The body weight of the animals was analyzed by two-way analysis of variance (ANOVA) with repeated measurements followed by Sidak's test. The data were expressed as mean \pm standard error of the mean (SEM) and analyzed with Student's *t* test (GraphPad Prism 7.0, San Diego, USA). For all analyses, the alpha value was considered 0.05.

Results

Exposure to MeHg Did Not Affect the Animals' Body Weight

No significant changes in the animals' body weight were found between the MeHg-exposed (239.9 ± 6.9 g) and control groups (237.3 ± 7.16 g; $p = 0.9883$) (Fig. 2).

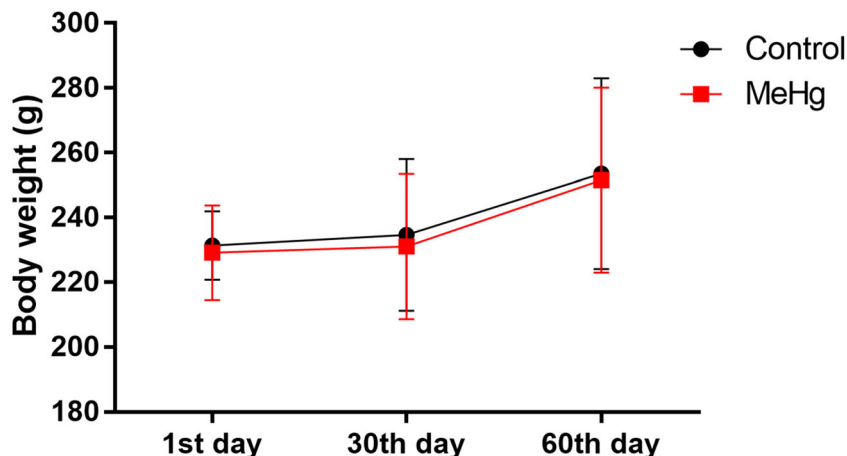
MeHg Exposure Promoted Lower Levels of GSH and TEAC and a Higher Concentration of TBARS in Blood

The GSH levels were significantly reduced ($p < 0.0001$) in the exposed ($59.71 \pm 2.18\%$) when compared to control groups ($100 \pm 4.7\%$) (Fig. 3a). It was also observed a significant ($p < 0.0001$) decrease in TEAC levels in the comparison between the exposed ($62.8 \pm 3.3\%$) and control groups ($100 \pm 2.57\%$) (Fig. 3b).

A significant increase in TBARS levels ($p < 0.0001$) was observed in animals exposed to MeHg ($194 \pm 5.7\%$) in comparison to those in the control group ($100 \pm 6.3\%$) (Fig. 3c).

The TBARS/TEAC ratio showed a significant increase in the exposed group ($304.8 \pm 13.38\%$) when compared to the control group ($100 \pm 9.7\%$), which indicates the occurrence of oxidative stress process (Fig. 3d).

Fig. 2 Body weight (g) (mean \pm SEM) of rats exposed to 0.04 mg/kg/day of MeHg for 60 days in comparison to the control group ($n = 30$)



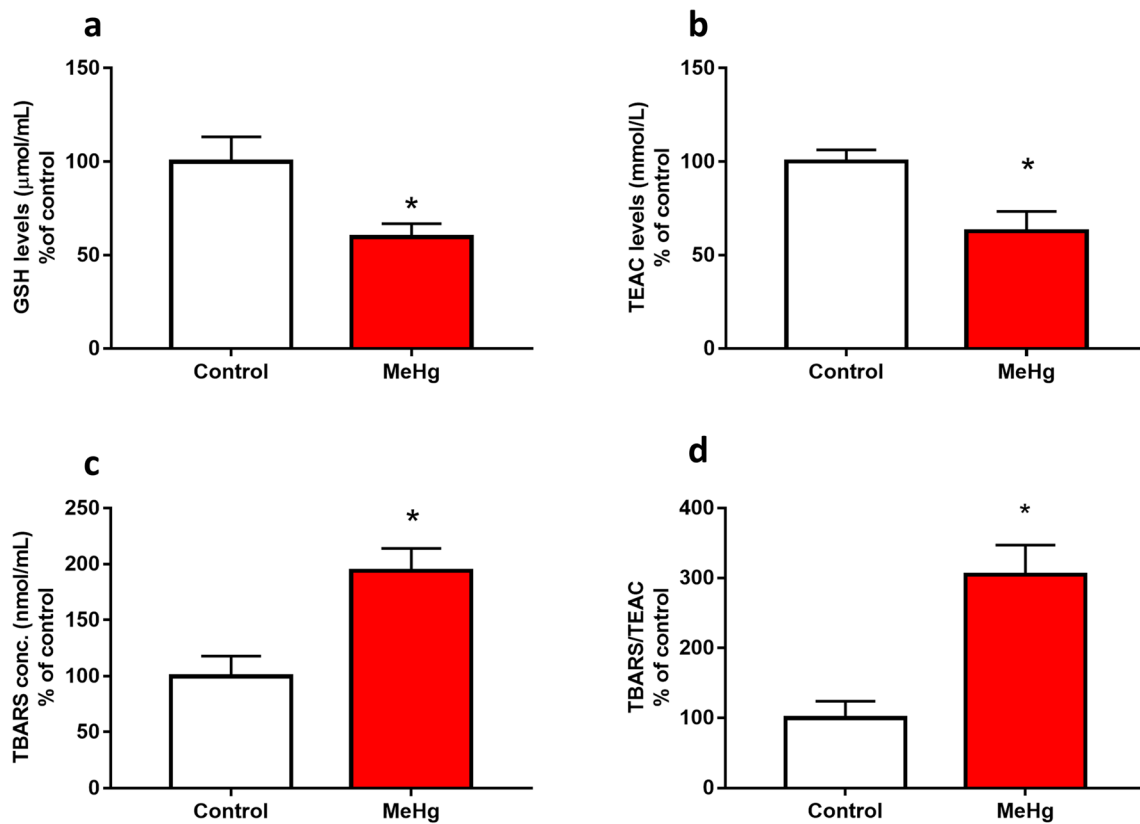


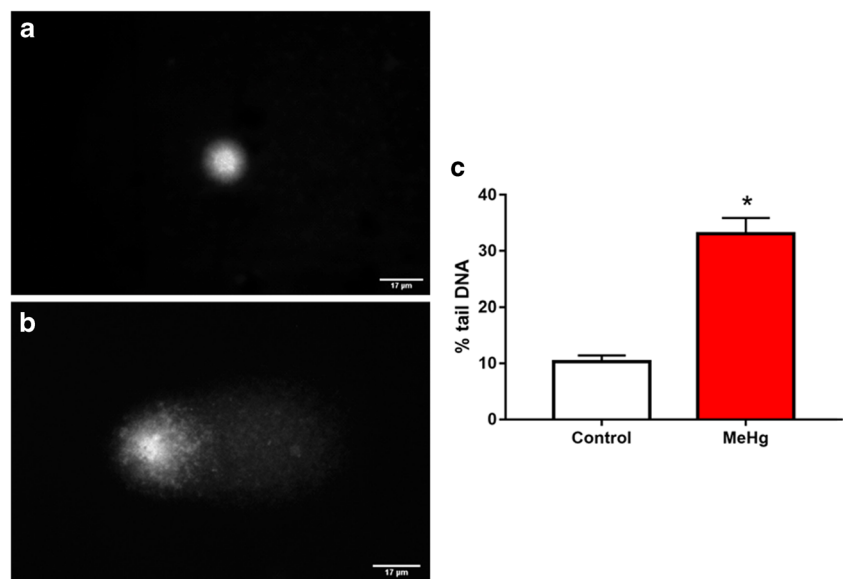
Fig. 3 Oxidative biochemistry analyses in blood after exposure to MeHg (0.04 mg/kg/day). The graphs show, as percentage of the control (Mean \pm SEM), the oxidative biochemistry results of both exposed and control

groups after the exposure period (60 days). **a** GSH ($\mu\text{mol/mL}$), **b** TEAC levels (mmol/L), **c** TBARS concentration (nmol/mL), and **d** TBARS/TEAC ratio. * $p < 0.05$ (Student's t test) ($n = 15$)

MeHg Long-Term Exposure Impaired DNA Integrity of Blood Cells

Animals exposed to MeHg ($33.0 \pm 1.0\%$) presented blood cells with a significantly larger tail ($p < 0.0001$) due to DNA fragmentation in comparison to the control group ($10.3 \pm 0.3\%$) (Fig. 4).

Fig. 4 **a, b** Comet assay photomicrographs obtained from rats' blood cells of control and MeHg-exposed groups submitted to DNA unwinding for 20 min and electrophoresis (30 V/cm, 300 mA) for 20 min. **c** Percentage of DNA damage in both control and MeHg-exposed groups ($n = 15$). * $p < 0.05$ (Student's t test). Scale bar: 17 μm



MeHg Exposure Increased Hg Level in Alveolar Bone

After 60 days, exposed animals presented a significantly higher total Hg level in the alveolar bone ($0.26 \pm 0.03 \mu\text{g/g}$) than the control group ($0.06 \pm 0.008 \mu\text{g/g}$; $p = 0.0002$) (Fig. 5).

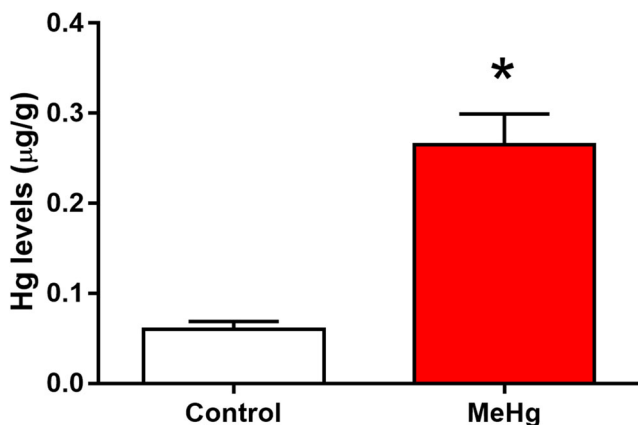


Fig. 5 Total Hg levels ($\mu\text{g/g}$) in the alveolar bone of animals exposed to 0.04 mg/kg/day of MeHg for 60 days and control group ($n = 15$). * $p < 0.05$ (Student's t test)

MeHg Exposure Promoted Morphological Changes in Alveolar Bone

Micro-CT analyses of alveolar bone from the MeHg-exposed group revealed significantly lower Tb.N (6.06 ± 0.21) in comparison to the control (7.08 ± 0.44 ; $p = 0.03$) (Fig. 6d). Significantly lower Tb.Th was also observed in the MeHg-exposed group (0.074 ± 0.001 mm) when compared to the control (0.08 ± 0.003 mm; $p = 0.006$) (Fig. 6e). Moreover, a significantly smaller bone volume fraction (BV/TV) was observed in the MeHg-exposed group ($46.98 \pm 1.62\%$) in comparison to the control ($55.47 \pm 1.81\%$; $p = 0.006$) (Fig. 6f).

MeHg Exposure Increased the Exposed Root Area on Second Molars

The analysis of the exposed root area on second molars (between CEJ and alveolar bone crest) indicated a significantly higher alveolar bone loss in the MeHg-exposed group (0.80 ± 0.01 mm²) when compared to the control (0.69 ± 0.02 mm²; $p = 0.006$) (Fig. 7).

Discussion

The findings of this research demonstrated that systemic, chronic, and low-dose exposure to MeHg in rats increases the levels of Hg in the alveolar bone and promotes microstructural changes that result in alveolar bone loss (in height). To the authors' best knowledge, this is a pioneering study on the damage susceptibility of alveolar bone exposed to MeHg.

In this animal study model, the long-term exposure to MeHg aimed to simulate the toxicological effects faced by populations in endemic areas. Our research group has previously reported that even 0.04 mg/kg/day of MeHg may damage several organs due to wide distribution of this organometallic compound [5, 10, 11, 33, 34]. From this perspective, the administration of MeHg by intragastric gavage aimed to simulate human exposure that mainly occurs by food ingestion [5, 10, 11]. Most of MeHg is absorbed by the enterocytes and is widely distributed to different systems through the blood, which is an important biomarker of exposure [35–38].

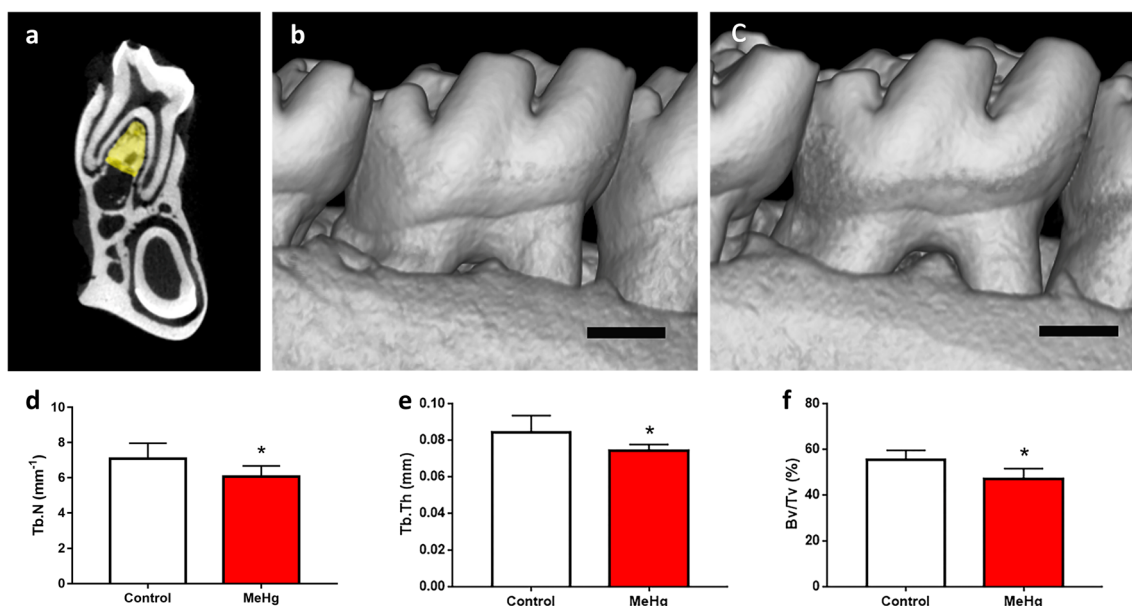
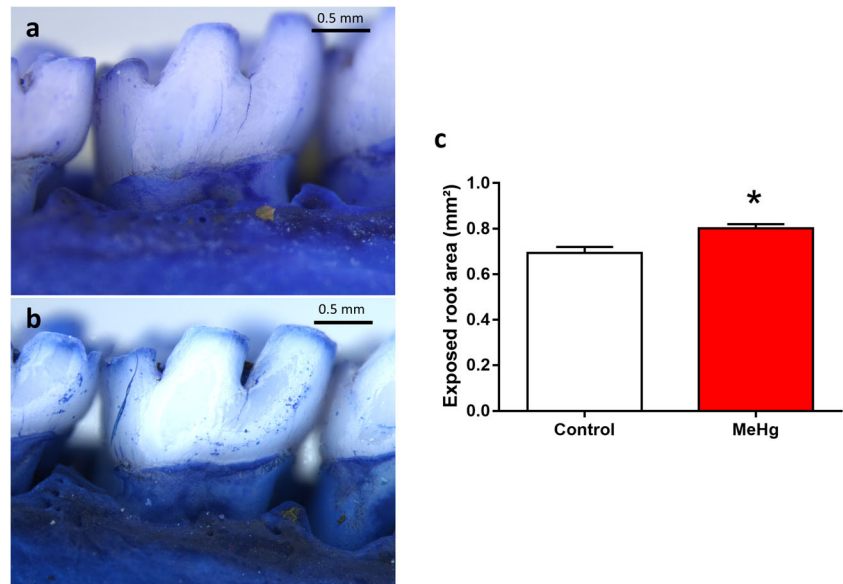


Fig. 6 a Representative micro-CT cross-sectional image of the region of interest (ROI): the mesial root of the lower second molar. b, c 3D image of the area of interest in the control and MeHg groups, respectively. d

Tb.N (mm^{-1}). e Tb.Th (mm). f BV/TV (%). The results are expressed as mean \pm SEM ($n = 15$). * $p < 0.05$ (Student's t test). Scale bar: 0.5 mm

Fig. 7 **a, b** Stereomicrographs of hemimandibles of the control and MeHg-exposed groups, respectively. **c** Graph of the exposed root area (mm^2) between CEJ and lingual alveolar bone crest of second molars ($n = 15$). * $p < 0.05$ (Student's *t* test). Scale bar: 0.5 mm



Although relevant data on Hg distribution kinetics have been reported [38], few descriptive pieces of evidence on Hg levels in exhumed human bones and rare studies on long bones are available in the literature [39–41], while research on the effects of Hg in the alveolar bone is still lacking. Therefore, this unprecedented *in vivo* study model demonstrates that after systemic administration of 0.04 mg/kg of MeHg for 60 days, the alveolar bone can incorporate 4 to 6 times more Hg than salivary glands and other regions of the central nervous system (CNS) [5, 10, 33, 34, 42].

Once absorbed in the bloodstream, Hg ions are able to enter the erythrocytes since the liposoluble characteristic of this organic form facilitates its passage through the lipid membranes into the cells [43, 44]. Due to its relatively high affinity to sulfhydryl groups (-SH), MeHg directly binds to several proteins and enzymes, promotes structural/functional alterations, and changes in molecular pathways that compromise cell homeostasis [45].

In order to validate this MeHg systemic exposure model, two important parameters were investigated: oxidative stress and DNA integrity [46]. The interaction between Hg and mitochondrial membrane changes disturbs intracellular ion homeostasis, affects the electron transport chain, and leads to overproduction of reactive oxygen species [47]. The cellular redox system becomes unbalanced due to the increase of ROS and consequent reduction of enzymatic antioxidant capacity; thus, this oxidative stress promotes the oxidation of several cellular biomolecules such as lipids, proteins, and DNA [4].

Several studies have already shown DNA damage after exposure to high doses of MeHg [48–51]; however, the results of this study evidenced damage to the genetic content of blood cells (expressed by DNA fragmentation) even after chronic exposure to daily low doses of MeHg. Although this study

aimed to validate the toxic effects resulting from MeHg oral administration, our findings also provide information to genotoxicity research. The direct connection of the toxic compound with DNA, alteration of DNA repair mechanisms, and inhibition of mitotic spindle formation are among the processes in which MeHg may lead to genotoxicity [46]. In addition, oxidative stress may exacerbate genotoxicity, since ROS can damage genetic material that impairs the activity of essential proteins for the cell cycle maintenance [52, 53]; thus, long-term DNA damages associated with changes in protein and enzyme activities may lead MeHg-induced apoptosis [54].

In addition to the genotoxic damage observed in this investigation, another mechanism of toxicity was evidenced through the analysis of oxidative biomolecular parameters: increase in TBARS and reduction in antioxidant capacity expressed by GSH and TEAC levels. The alteration in cellular redox balance was confirmed by the TBARS/TEAC ratio, which demonstrated an increase in pro-oxidative factors in comparison to antioxidant defenses. The TBARS concentration indicated an increase in MDA, which is a metabolite derived from the LPO of polyunsaturated fatty acids in cell membranes and an important indicator of oxidative stress [55]. The increase in LPO levels was also reported in other studies with MeHg exposure at different dosages [56–59].

In addition to intracellular ROS increase, MeHg triggers reactions on antioxidant compounds such as GSH, which is the most abundant non-protein thiol compound [60] and acts as the first defense against Hg ions [61]; however, this protective effect can decrease GSH concentration and cells become more vulnerable to ROS that are no longer inactivated [61]. It is important to highlight that MeHg toxicity is a result of accumulation through interactions with intracellular biomolecules [45], and this fact was evidenced in this study by the presence of high levels of Hg ions in alveolar bone tissue.

Since these findings demonstrated the toxicity resulted from the intracellular presence of Hg and transportation through the bloodstream [44], its effect on other tissues such as bone can be assumed. Nevertheless, only few studies have evaluated the MeHg effects on bone tissue, since it exhibits less bioaccumulation when compared to the CNS [16, 62, 63]. A controlled model study revealed that acute MeHg exposure alters both osteoclasts and osteoblast metabolism and calcium homeostasis [29].

In this context, the effects of MeHg exposure on alveolar bone tissue are still not reported in the literature. This tissue is one component of the periodontium that forms the primary support structure of teeth and present different characteristics when compared to other bones. Unlike bones of the trunk, which derive from endochondral ossification, the alveolar bone begins its formation from ectomesenchymal cells of the tooth germ simultaneously with cementum and periodontal ligament [18, 21].

Oxidative changes have been associated with the modulation of the resorption dynamics of the alveolar bone. Studies demonstrate that this oxidative imbalance can culminate in the imbalance of inflammatory reaction mechanisms, altering cell physiological maintenance, favoring cell death [64, 65]. In periodontal tissue, both the formation and removal of ROS can be observed by increasing the loss of support tissues through the modulation of bone metabolism. The literature points out that modulation involves changes in osteoblastic formation and osteoclastic bone resorption, favoring bone loss [65].

Differently from long bones, the particular morphology of the alveolar bone presents a compact structure with wide plate-like trabeculae that increase mineral density and bone volume fraction [18]; thus, parameters of microstructure damage were investigated in this study. Currently, tridimensional micro-CT is the gold-standard, non-destructive, sensitive, and effective tool for morphological analysis of several alveolar bone parameters such as Tb.N, Tb.Th, and BV/TV [66]. The micro-CT analysis revealed that alveolar bone was susceptible to damage after MeHg exposure at low doses over a long period. Although not considered a target organ for Hg accumulation [15], high levels of this metal were found in the alveolar bone. This finding corroborates with the cytotoxic potential of Hg, which has a systemic influence on the body metabolism that changes the alveolar bone structure even at low doses.

Exposure to MeHg was able to alter both Tb.N and Tb.Th, which in turn decreased the BV/TV. The larger exposed root areas observed in the second molars indicate that potential metabolic changes impaired bone remodeling and the quality of alveolar bone produced by osteoblasts. This mechanism may be associated with the affinity between Hg and -SH groups present in several cellular proteins [45] such as type I and III collagen, sialoprotein, and osteopontin, which are directly involved in bone tissue maintenance [67].

Changes in these microtomographic parameters may indicate alterations in the physical and structural properties of alveolar bone tissue [68]. Depending on the stimulus type, molecular events that regulate bone tissue formation and remodeling may cause metabolic imbalance and change the ultrastructural organization that becomes clinically visible as alveolar bone loss [69]. The exposed root area found in animals exposed to MeHg in this study was similar to the height loss observed in periodontitis [70, 71], which indicates that microstructural changes can decrease the vertical dimension of the alveolar bone.

Therefore, the findings of this study contribute to the identification of the morphological toxic effects of MeHg on the alveolar bone of rats in a model of systemic exposure at low doses. Future investigations about the damage mechanisms in the interaction process between Hg ions and bone metabolism are necessary.

Conclusion

Long-term MeHg exposure at low doses increased Hg levels in the alveolar bone, induced microstructural changes, and resulted in alveolar bone loss (in height). These findings may represent an important translational significance for the oral health of subjects environmentally exposed to MeHg due to a potential risk indicator for the development of periodontal diseases.

Funding This work was supported by the Brazilian National Council for Scientific and Technological Development (CNPq), Fundação de Amparo a Pesquisa do Estado do Pará (FAPESPA), and Pró-Reitoria de Pesquisa e Pós-Graduação da UFPA (PROPEP, UFPA, Brazil).

Compliance with Ethical Standards

All procedures were previously approved by Ethics committee on animal experimentation by Federal University of Para (BIO 225-14-CEPAE-UFPA) following the guidelines suggested by NIH Guide to Care and Use of Laboratory Animals.

Competing Interest The authors declare no conflicts of interest in the study.

References

1. Organization WH (2013) Mercury and health (fact sheet no. 361). Geneva
2. Hong Y-S, Kim Y-M, Lee K-E (2012) Methylmercury exposure and health effects. *J Prev Med Public Health* 45(6):353. <https://doi.org/10.3961/jpmph.2012.45.6.353>
3. Bernhoft RA (2012) Mercury toxicity and treatment: a review of the literature. *J Environ Public Health* 2012. <https://doi.org/10.1155/2012/460508>
4. Antunes A, Ferrer B, Marques Gonçalves F, Tsatsakis AM, Renieri EA, Skalny AV, Farina M, Rocha JB, Aschner M (2018) Oxidative

- stress in methylmercury-induced cell toxicity. *J Toxics* 6(3):47. <https://doi.org/10.3390/toxics6030047>
5. Bittencourt LO, Puty B, Charone S, Aragão WAB, Farias-Junior PM, Silva MCF, Crespo-Lopez ME, Leite AL, Buzalaf MAR, Lima RR (2017) Oxidative biochemistry disbalance and changes on proteomic profile in salivary glands of rats induced by chronic exposure to methylmercury. *J Oxidative Med Cell Longev* 2017:1–15. <https://doi.org/10.1155/2017/5653291>
 6. Crespo-Lopez ME, Costa-Malaquias A, Oliveira EH, Miranda MS, Arrifano GP, Souza-Monteiro JR, Espirito-Santo Sagica F, Fontes-Junior EA, Maia CS, Macchi BM (2016) Is low non-lethal concentration of methylmercury really safe? A report on genotoxicity with delayed cell proliferation. *PLoS One* 11(9). <https://doi.org/10.1371/journal.pone.0162822>
 7. Nogueira LS, Vasconcelos CP, Mitre GP, da Silva Kataoka MS, Lima MO, de Oliveira EH, Lima RR (2019) Oxidative damage in human periodontal ligament fibroblast (hPLF) after methylmercury exposure. *J Oxidative Med Cell Longev* 2019:1–7. <https://doi.org/10.1155/2019/8470857>
 8. Arrifano GP, Martín-Doimeadios RCR, Jiménez-Moreno M, Ramírez-Mateos V, da Silva NF, Souza-Monteiro JR, Augusto-Oliveira M, Paraense RS, Macchi BM, do Nascimento JLM (2018) Large-scale projects in the amazon and human exposure to mercury: the case-study of the Tucuruí dam. *J Ecotoxicol Environ Saf* 147:299–305. <https://doi.org/10.1016/j.ecoenv.2017.08.048>
 9. Crespo-López ME, Macêdo GL, Arrifano GP, Maria da Conceição NP, do Nascimento JLM, Herculano AM (2011) Genotoxicity of mercury: contributing for the analysis of Amazonian populations. *J Environ Int* 37(1):136–141. <https://doi.org/10.1016/j.envint.2010.08.009>
 10. Lima LA, Bittencourt LO, Puty B, Fernandes RM, Nascimento PC, Silva MCF, Alves-Junior SM, Pinheiro JJV, Lima RR (2018) Methylmercury intoxication promotes metallothionein response and cell damage in salivary glands of rats. *J Biol Trace Elem Res* 185(1):135–142. <https://doi.org/10.1007/s12011-017-1230-9>
 11. Farias-Junior PMA, Teixeira FB, Fagundes NCF, Miranda GHN, Bittencourt LO, de Oliveira Paraense RS, Silva MCF, Santo Sagica FE, de Oliveira EH, Crespo-López ME (2017) Chronic intoxication by methylmercury leads to oxidative damage and cell death in salivary glands of rats. *Metallomics* 9(12):1778–1785. <https://doi.org/10.1039/c7mt00168a>
 12. Kim K-H, Kabir E, Jahan SA (2016) A review on the distribution of Hg in the environment and its human health impacts. *J Hazard Mater* 306:376–385. <https://doi.org/10.1016/j.jhazmat.2015.11.031>
 13. Fernandes Azevedo B, Barros Furieri L, Peçanha FM, Wiggers GA, Frizera Vassallo P, Ronacher Simões M, Fiorim J, Rossi de Batista P, Fiorese M, Rossoni L (2012) Toxic effects of mercury on the cardiovascular and central nervous systems. *J BioMed Res Int* 2012. <https://doi.org/10.1155/2012/949048>
 14. Schuurs A (1999) Reproductive toxicity of occupational mercury. A review of the literature. *J Dent* 27(4):249–256. [https://doi.org/10.1016/s0300-5712\(97\)00039-0](https://doi.org/10.1016/s0300-5712(97)00039-0)
 15. Suzuki N, Yamamoto M, Watanabe K, Kambegawa A, Hattori A (2004) Both mercury and cadmium directly influence calcium homeostasis resulting from the suppression of scale bone cells: the scale is a good model for the evaluation of heavy metals in bone metabolism. *J Bone Miner Metab* 22(5):439–446. <https://doi.org/10.1007/s00774-004-0505-3>
 16. Yachiguchi K, Sekiguchi T, Nakano M, Hattori A, Yamamoto M, K-i K, Maeda M, Tabuchi Y, Kondo T, Kamauchi H (2014) Effects of inorganic mercury and methylmercury on osteoclasts and osteoblasts in the scales of the marine teleost as a model system of bone. *J Zool Sci* 31(5):330–337. <https://doi.org/10.2108/zs130265>
 17. Abd El-Aziz GS, El-Fark MM, Saleh HA (2012) The prenatal toxic effect of methylmercury on the development of the appendicular skeleton of rat fetuses and the protective role of vitamin E. *Anat Rec (Hoboken)* 295(6):939–949. <https://doi.org/10.1002/ar.22485>
 18. Zhou S, Yang Y, Ha N, Zhang P, Ma X, Gong X, Hong Y, Yang X, Yang S, Dai Q (2018) The specific morphological features of alveolar bone. *J Craniofacial Surg* 29(5):1216–1219. <https://doi.org/10.1097/scs.00000000000004395>
 19. Rawlinson S, Boyde A, Davis G, Howell P, Hughes F, Kingsmill VJ (2009) Ovariectomy vs. hypofunction: their effects on rat mandibular bone. *88(7):615–620*
 20. Passos-Soares JS, Vianna MIP, Gomes-Filho IS, Cruz SS, Barreto ML, Adan LF, Rösing CK, Trindade SC, Cerqueira EM, Scannapieco FA (2017) Association between osteoporosis treatment and severe periodontitis in postmenopausal women. *24(7):789–795*
 21. Fleischmannova J, Matalova E, Sharpe P, Miskic I, Radlanski R (2010) Formation of the tooth-bone interface. *J Dental Res* 89(2):108–115. <https://doi.org/10.1177/0022034509355440>
 22. Kong H-K, Wong M-H, Chan H-M, Lo SC-L (2013) Chronic exposure of adult rats to low doses of methylmercury induced a state of metabolic deficit in the somatosensory cortex. *J Proteome Res* 12(11):5233–5245. <https://doi.org/10.1021/pr400356v>
 23. Ellman G (1959) Tissue sulfhydryl groups. *Arch Biochem Biophys* 82(1):70–77. [https://doi.org/10.1016/0003-9861\(59\)90090-6](https://doi.org/10.1016/0003-9861(59)90090-6)
 24. Rufino M, Alves R, Britoetal E (2007) Determination of the total antioxidant activity in fruits by the capture of free radical DPPH. *J Press Release Embrapa* 127:1–4
 25. Re R, Pellegrini N, Proteggente A, Pannala A, Yang M, Rice-Evans C (1999) Antioxidant activity applying an improved ABTS radical cation decolorization assay. *J Free Radic Biol Med* 26(9–10):1231–1237. [https://doi.org/10.1016/s0891-5849\(98\)00315-3](https://doi.org/10.1016/s0891-5849(98)00315-3)
 26. Kohn HI, Liversedge M (1944) On a new aerobic metabolite whose production by brain is inhibited by apomorphine, emetine, ergotamine, epinephrine, and menadione. *J Pharmacol Exp Ther* 82(3):292–300
 27. Percário S (1994) Dosagem das LDLs modificadas através da peroxidação lipídica: correlação com o risco aterogênico. *Anais Médicos dos Hospitais e da Faculdade de Ciências Médicas da Santa Casa de São Paulo* 13(49–52):7–9
 28. Singh N, Stephens R (1997) Microgel electrophoresis: sensitivity, mechanisms, and DNA electrostretching. *J Mutat Res/DNA Repair* 383(2):167–175. [https://doi.org/10.1016/s0921-8777\(96\)00056-0](https://doi.org/10.1016/s0921-8777(96)00056-0)
 29. Suzuki T, Akagi H, Arimura K, Ando T, Sakamoto M, Satoh H, Nagamura A, Futatsuka M, Matsuyama A (2004) Mercury analysis manual. Ministry of the Environment, Japan
 30. Hassumi JS, Mulinari-Santos G, Fabris ALS, Jacob RGM, Gonçalves A, Rossi AC, Freire AR, Faverani LP, Okamoto R (2018) Alveolar bone healing in rats: micro-CT, immunohistochemical and molecular analysis. 26
 31. Liberman DN, Pilau RM, Orlandini LF, Gaio EJ, Rösing CK (2011) Comparison of two methods for alveolar bone loss measurement in an experimental periodontal disease model in rats. *J Braz Oral Res* 25(1):80–84. <https://doi.org/10.1590/S1806-83242011005000002>
 32. Bannach SV, Teixeira FB, Fernandes LMP, Ferreira RO, Santana LNS, Fontes-Júnior EA, Oliveira GB, Prediger RD, Maia CSF, Lima RR (2015) Alveolar bone loss induced by chronic ethanol consumption from adolescence to adulthood in Wistar rats. *Indian J Exp Biol*
 33. Santana LNS, Bittencourt LO, Nascimento PC, Fernandes RM, Teixeira FB, Fernandes LMP, Silva MCF, Nogueira LS, Amado LL, Crespo-Lopez ME (2019) Low doses of methylmercury exposure during adulthood in rats display oxidative stress, neurodegeneration in the motor cortex and lead to impairment of motor skills. *J Trace Elem Med Biol* 51:19–27. <https://doi.org/10.1016/j.jtemb.2018.09.004>

34. Freire MAM, Santana LNS, Bittencourt LO, Nascimento PC, Fernandes RM, Leão LKR, Fernandes LMP, Silva MCF, Amado LL, Gomes-Leal W (2019) Methylmercury intoxication and cortical ischemia: pre-clinical study of their comorbidity. *J Ecotoxicol Environ Saf* 174:557–565. <https://doi.org/10.1016/j.ecoenv.2019.03.009>
35. Clarkson TW (2002) The three modern faces of mercury. *J Environ Health Perspect* 110(suppl 1):11–23. <https://doi.org/10.1289/ehp.02110s111>
36. Foulkes E (2000) Transport of toxic heavy metals across cell membranes (44486). *J Proc Soc Exp Biol Med* 223(3):234–240. <https://doi.org/10.1177/153537020022300304>
37. Ye B-J, Kim B-G, Jeon M-J, Kim S-Y, Kim H-C, Jang T-W, Chae H-J, Choi W-J, Ha M-N, Hong Y-S (2016) Evaluation of mercury exposure level, clinical diagnosis and treatment for mercury intoxication. *J Ann Occup Environ Med* 28(1). <https://doi.org/10.1186/s40557-015-0086-8>
38. Branco V, Caito S, Farina M, Teixeira da Rocha J, Aschner M, Carvalho C (2017) Biomarkers of mercury toxicity: past, present, and future trends. *J Toxicol Environ Health, Part B* 20(3):119–154. <https://doi.org/10.1080/10937404.2017.1289834>
39. Rasmussen KL, Boldsen JL, Kristensen HK, Skytte L, Hansen KL, Møhlholm L, Grootes PM, Nadeau M-J, Eriksen KMF (2008) Mercury levels in Danish medieval human bones. *J Archaeol Sci* 35(8):2295–2306. <https://doi.org/10.1016/j.jas.2008.03.003>
40. Yamada M-o, Tohno S, Tohno Y, Minami T, Ichii M, Okazaki Y (1995) Accumulation of mercury in excavated bones of two natives in Japan. *J Sci Total Environ* 162(2–3):253–256. [https://doi.org/10.1016/0048-9697\(95\)04435-4](https://doi.org/10.1016/0048-9697(95)04435-4)
41. Lindh U, Brune D, Nordberg G, Wester P-O (1980) Levels of antimony, arsenic, cadmium, copper, lead, mercury, selenium, silver, tin and zinc in bone tissue of industrially exposed workers. *J Sci Total Environ* 16(2):109–116. [https://doi.org/10.1016/0048-9697\(80\)90018-2](https://doi.org/10.1016/0048-9697(80)90018-2)
42. Bittencourt LO, Dionizio A, Nascimento PC, Puty B, Leão LKR, Luz DA, Silva MCF, Amado LL, Leite A, Buzalaf MR (2019) Proteomic approach underlying the hippocampal neurodegeneration caused by low doses of methylmercury after long-term exposure in adult rats. *J Metallomics* 11(2):390–403. <https://doi.org/10.1039/c8mt00297e>
43. Bradley MA, Barst BD, Basu N (2017) A review of mercury bio-availability in humans and fish. *Int J Environ Res Public Health* 14(2):169. <https://doi.org/10.3390/ijerph14020169>
44. Ynalvez R, Gutierrez J, Gonzalez-Cantu H (2016) Mini-review: toxicity of mercury as a consequence of enzyme alteration. *J Biomaterials* 29(5):781–788. <https://doi.org/10.1007/s10534-016-9967-8>
45. Farina M, Aschner M (2019) Glutathione antioxidant system and methylmercury-induced neurotoxicity: an intriguing interplay. *Biochim Biophys Acta, Gen Subj* 1863(12):129285. <https://doi.org/10.1016/j.bbagen.2019.01.007>
46. Crespo-López ME, Macêdo GL, Pereira SI, Arrifano GP, Picanço-Diniz DL, do Nascimento JLM, Herculano AM (2009) Mercury and human genotoxicity: critical considerations and possible molecular mechanisms. *J Pharmacol Res* 60(4):212–220. <https://doi.org/10.1016/j.phrs.2009.02.011>
47. Liu W, Yang T, Xu Z, Xu B, Deng Y (2019) Methyl-mercury induces apoptosis through ROS-mediated endoplasmic reticulum stress and mitochondrial apoptosis pathways activation in rat cortical neurons. *Free Radic Res* 53(1):26–44. <https://doi.org/10.1080/10715762.2018.1546852>
48. Silva de Paula E, Carneiro MFH, Grotto D, Hernandez LC, Antunes LMG, Barbosa F Jr (2016) Protective effects of niacin against methylmercury-induced genotoxicity and alterations in antioxidant status in rats. *J Toxicol Environ Health, Part A* 79(4):174–183. <https://doi.org/10.1080/15287394.2015.1137264>
49. Grotto D, Barcelos GR, Valentini J, Antunes LM, Angeli JP, Garcia SC, Barbosa F Jr (2009) Low levels of methylmercury induce DNA damage in rats: protective effects of selenium. *Arch Toxicol* 83(3):249–254. <https://doi.org/10.1007/s00204-008-0353-3>
50. Kirkpatrick M, Benoit J, Everett W, Gibson J, Rist M, Fredette N (2015) The effects of methylmercury exposure on behavior and biomarkers of oxidative stress in adult mice. *Neurotoxicology* 50:170–178. <https://doi.org/10.1016/j.neuro.2015.07.001>
51. Barcelos GR, Angeli JP, Serpeloni JM, Grotto D, Rocha BA, Bastos JK, Knasmüller S, Júnior FB (2011) Quercetin protects human-derived liver cells against mercury-induced DNA-damage and alterations of the redox status. *Mutat Res* 726(2):109–115. <https://doi.org/10.1016/j.mrgentox.2011.05.011>
52. Chen N, Lin M, Liu N, Wang S, Xiao X (2019) Methylmercury-induced testis damage is associated with activation of oxidative stress and germ cell autophagy. *J Inorg Biochem* 190:67–74. <https://doi.org/10.1016/j.jinorgbio.2018.10.007>
53. Silva-Pereira LC, da Rocha CA, Cunha LR, da Costa ET, Guimarães AP, Pontes TB, Diniz DL, Leal MF, Moreira-Nunes CA, Burbano RR (2014) Protective effect of prolactin against methylmercury-induced mutagenicity and cytotoxicity on human lymphocytes. *Int J Environ Res Public Health* 11(9):9822–9834. <https://doi.org/10.3390/ijerph110909822>
54. Wang X, Yan M, Zhao L, Wu Q, Wu C, Chang X, Zhou Z (2016) Low-dose methylmercury-induced apoptosis and mitochondrial DNA mutation in human embryonic neural progenitor cells. *Oxidative Med Cell Longev* 2016:5137042–5137010. <https://doi.org/10.1155/2016/5137042>
55. Ohkawa H, Ohishi N, Yagi K (1979) Assay for lipid peroxides in animal tissues by thiobarbituric acid reaction. *Anal Biochem* 95(2):351–358. [https://doi.org/10.1016/0003-2697\(79\)90738-3](https://doi.org/10.1016/0003-2697(79)90738-3)
56. Joshi D, Kumar MD, Kumar SA, Sangeeta S (2014) Reversal of methylmercury-induced oxidative stress, lipid peroxidation, and DNA damage by the treatment of N-acetyl cysteine: a protective approach. *J Environ Pathol Toxicol Oncol* 33(2). <https://doi.org/10.1615/jenviropatholtoxiconcol.2014010291>
57. Pal M, Ghosh M (2012) Prophylactic effect of alpha-linolenic acid and alpha-eleostearic acid against MeHg induced oxidative stress, DNA damage and structural changes in RBC membrane. *Food Chem Toxicol* 50(8):2811–2818. <https://doi.org/10.1016/j.fct.2012.05.038>
58. Lu TH, Hsieh SY, Yen CC, Wu HC, Chen KL, Hung DZ, Chen CH, Wu CC, Su YC, Chen YW, Liu SH, Huang CF (2011) Involvement of oxidative stress-mediated ERK1/2 and p38 activation regulated mitochondria-dependent apoptotic signals in methylmercury-induced neuronal cell injury. *Toxicol Lett* 204(1):71–80. <https://doi.org/10.1016/j.toxlet.2011.04.013>
59. Huang CF, Liu SH, Hsu CJ, Lin-Shiau SY (2011) Neurotoxicological effects of low-dose methylmercury and mercuric chloride in developing offspring mice. *Toxicol Lett* 201(3):196–204. <https://doi.org/10.1016/j.toxlet.2010.12.016>
60. Dickinson DA, Forman HJ (2002) Cellular glutathione and thiols metabolism. *Biochem Pharmacol* 64(5–6):1019–1026. [https://doi.org/10.1016/s0006-2952\(02\)01172-3](https://doi.org/10.1016/s0006-2952(02)01172-3)
61. Sarafian TA (1999) Methylmercury-induced generation of free radicals: biological implications. *Met Ions Biol Syst* 36:415–444
62. Berglund M, Åkesson A, Bjellerup P, Vahter M (2000) Metal–bone interactions. *J Toxicol Lett* 112:219–225. [https://doi.org/10.1016/S0378-4274\(99\)00272-6](https://doi.org/10.1016/S0378-4274(99)00272-6)
63. Nagashima K, Fujii Y, Tsukamoto T, Nukuzuma S, Satoh M, Fujita M, Fujioka Y, Akagi H (1995) Apoptotic process of cerebellar degeneration in experimental methylmercury intoxication of rats. *J Acta Neuropathol* 91(1):72–77. <https://doi.org/10.1007/s004010050394>

64. Ryter SW, Kim HP, Hoetzel A, Park JW, Nakahira K, Wang X, Choi AMJA, signaling r (2007) Mechanisms of cell death in oxidative stress. *9*(1):49–89
65. Lopes Castro MM, Nascimento PC, Souza-Monteiro D, Santos SM, Arouck MB, Garcia VB, Araújo RF, de Araujo AA, Balbinot GS, Collares FM (2020) Blood oxidative stress modulates alveolar bone loss in chronically stressed rats. *21*(10):3728
66. Argenta MA, Buriol TM, Hecke MB (2010) Metodologia para a obtenção de parâmetros físicos e geométricos do osso trabecular função de imagens de micro tomografia. In: XXXI Iberian-Latin-American Congress on Computational Methods in Engineering. pp. 15–18
67. Nanci A (1999) Content and distribution of noncollagenous matrix proteins in bone and cementum: relationship to speed of formation and collagen packing density. *J Struct Biol* *126*(3):256–269. <https://doi.org/10.1006/jsbi.1999.4137>
68. Silva A, Boyd S, Manske S, Alves J, de Carvalho J (2019) Assessment of the elastic properties of human vertebral trabecular bone using computational mechanical tests and x-ray microtomography—a subvolume analysis. *J Biomed Phys Eng Express* *5*(4):045031. <https://doi.org/10.1088/2057-1976/ab2c70>
69. Sodek J, Mckee MD (2000) Molecular and cellular biology of alveolar bone. *J Periodontol* *24*(1):99–126. <https://doi.org/10.1034/j.1600-0757.2000.2240106.x>
70. Fernandes MI, Gaio EJ, Oppermann RV, Rados PV, Rosing CK (2007) Comparison of histometric and morphometric analyses of bone height in ligature-induced periodontitis in rats. *Braz Oral Res* *21*(3):216–221. <https://doi.org/10.1590/S1806-83242007000300005>
71. CHO MI, Garant PR (2000) Development and general structure of the periodontium. *J Periodontol* *24*(1):9–27. <https://doi.org/10.1034/j.1600-0757.2000.2240102.x>

Publisher's Note Springer Nature remains neutral with regard to jurisdictional claims in published maps and institutional affiliations.